Preparation, Thermal Properties, and T_g Increase Mechanism of Poly(acetoxystyrene-*co*-octavinyl-polyhedral oligomeric silsesquioxane) Hybrid Nanocomposites

Hongyao Xu,* Benhong Yang, Jiafeng Wang, Shanyi Guang, and Cun Li

School of Chemistry and Chemical Engineering & Key Laboratory of Environment-friendly Polymer Materials of Anhui Province, Anhui University, Hefei 230039, China

Received July 28, 2005; Revised Manuscript Received October 3, 2005

ABSTRACT: A series of poly(acetoxystyrene-*co*-octavinyl-polyhedral oligomeric silsesquioxane) (PAS−POSS) hybrid nanocomposites were synthesized by free radical polymerization and characterized by FTIR, ^{1}H NMR, GPC, DSC, and TGA technologies. The POSS contents in these nanocomposites were calculated on the basis of FTIR data. The results show that POSS content can be controlled by varying the POSS feed ratios. DSC and TGA measurements reveal that the incorporation of POSS into polymers can improve the thermal properties of polymeric materials. The FTIR spectra were employed to explain the T_g improvement mechanism. POSS moieties influence the T_g of nanocomposite in two ways. At relatively low POSS contents, POSS plays a role of inert diluent to reduce T_g. With the increase of POSS contents, both the aggregation of POSS nanoparticles and the dipole−dipole interaction between POSS and PAS molecules contribute to the increase of T_g.

Introduction

Inorganic−organic hybrid polymers have attracted great interest recently because of their better performance in thermal stability and oxidative resistance compared to their mother homogeneous polymers.[1] A typical hybrid material will contain an organic phase bound covalently with inorganic moieties.[2]

Polyhedral oligomeric silsesquioxane (POSS) is a class of inorganic compounds that has a well-defined structure with a silica-like core (Si_8O_{12}) surrounded by eight organic corner groups (functional or inert).[3] The functional corner groups enable POSS to copolymerize with organic monomers, such as acrylates,[4] styrenes,[2,5] norbornenes,[3] epoxy,[6,7] siloxane,[8,9] urethane,[10,11] and so on. The incorporation of nanosize POSS cores into a polymer matrix can result in significant improvements in a variety of physical and mechanical properties.[12] Because of the excellent properties brought by odorless and environment-friendly POSS chemicals, studies related to POSS-based hybrid polymers have undergone an approximately exponential growth since the first technical publication on POSS polymers in 1991.[13] However, those previous researches were mostly limited to the linear or pendent polymeric systems using POSS macromers with only a single functional corner group.[2−7,10−18] Therefore, some researchers are shifting their interests toward star or network hybrid polymers with more than two functional groups on POSS corners, and many efforts have been made so far.[19−26] However, these works were mainly about the preparation of these hybrid polymers, and properties of these star or network polymers were little discussed.[27] In this paper, we will report the synthesis and characterization of octavinyl-POSS-based hybrid polymers with star-type structure as well as the thermal properties and the possible T_g enhancment mechanism.

* Corresponding author: Tel +86-551-5107342; Fax +86-551-5108203; e-mail hongyaoxu@163.com.

Scheme 1. Formation of PAS−POSS Hybrid Nanocomposites with Star Structure via Free Radical Polymerization

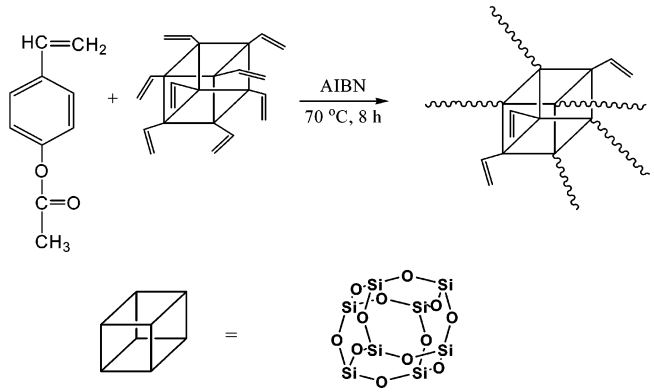

Experimental Section

Materials. Octavinyl-polyhedral oligomeric silsesquioxane (POSS) monomers were synthesized according to the procedures described in ref 28. Acetoxystyrene was purchased from Aldrich, distilled from calcium hydride under reduced pressure, and stored in sealed ampules in a refrigerator. Azobis(isobutyronitrile) (AIBN) was refined in heated ethanol and kept in a dried box. Spectroscopy-grade THF and 1,4-dioxane were dried over 4 Å molecular sieves and distilled from sodium benzophenone ketyl immediately prior to use. All other solvents were used as received.

Polymerization. The polymerization reactions were carried out under nitrogen protection using a vacuum-line system. Poly(acetoxystyrene-*co*-octavinyl-POSS)s were prepared by a conventional free radical polymerization technique, as shown in Scheme 1. For comparison, the homopolyacetoxystyrene (PAS) was also synthesized. In a typical reaction, 9.86 mmol of acetoxystyrene and 0.14 mmol of POSS monomer in 5 mL of dried 1,4-dioxane were polymerized using the AIBN initiator (1 wt % based on monomer) at 70 °C under a nitrogen atmosphere for 8 h. The product then was poured into excessive cyclohexane under vigorously agitation to dissolve the unreacted monomers and precipitate the nanocomposite. A 59.7 wt % yield was obtained through this procedure. The crude product was redissolved in THF to form a homogeneous

10.1021/ma0516687 CCC: $30.25
Published on Web 11/16/2005

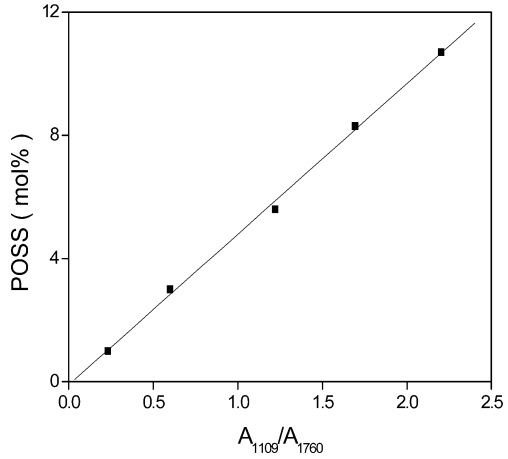

Figure 1. IR calibration curve for determining POSS contents in PAS−POSS nanocomposites.

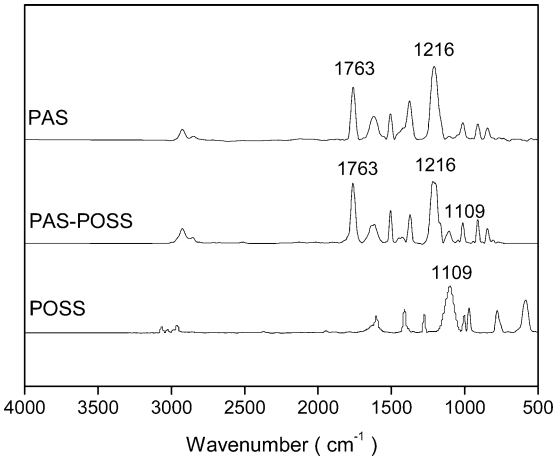

Figure 2. FTIR spectra of pure POSS, PAS, and PAS−POSS nanocomposites.

and transparent solution. This solution was then added dropwisely into cyclohexane. This purification procedure was repeated twice to ensure that the POSS and acetoxystyrene monomers were removed thoroughly.

Instrumentation. FTIR spectra were measured with a Nicolet NEXUS 870 FTIR spectrophotometer using KBr powder at room temperature. ^{1}H NMR spectra were recorded on a Bruker AVANCE/DMX 300 spectrometer using chloroform-*d* solvent. Weight-average (M_w) and number-average (M_n) molecular weights and polydispersity index (PDI, M_w/M_n) were determined by a Waters 515 gel permeation chromatograph (GPC). Differential scanning calorimetry (DSC) was performed on a TA Instruments DSC 9000 equipped with a liquid nitrogen cooling accessory (LNCA) unit under a continuous nitrogen purge (50 mL/min). The scan rate was 20 °C/min within the temperature range 30−300 °C. The sample was quickly cooled to 0 °C from the melt for the first scan and then scanned from 20 to 250 °C at 10 °C/min. The glass-transition temperature (T_g) was taken as the midpoint of the specific heat increment. Thermogravimetric analysis was carried out using a TA Instruments TGA 2050 thermogravimetric analyzer with a heating rate of 20 °C/min from 25 to 700 °C under a continuous nitrogen purge (100 mL/min). The thermal degradation temperature (T_{dec}) was defined as the temperature of 5% weight loss.

Determination of POSS Content.[29] Since the characteristic absorption peaks of POSS and PAS, which are respectively located at 1109 and 1760 cm^{-1}, are not interfered or overlapped with each other, the FTIR spectra are used to determine the POSS contents in the hybrids. A series of PAS/POSS mixtures with different molar ratios were first dissolved in THF to ensure intimate mixing and then cast into a thin film for FTIR testing. Using the strong absorption band of the carbonyl group in the PAS chains at 1760 cm^{-1} as an internal standard, we plotted the ratios of areas of absorption bands (A_{1109}/A_{1760}) against the POSS molar contents in the mixtures, and a calibration curve was obtained (shown in Figure 1). The POSS molar percentage (Y_{POSS}) held a linear relationship with A_{1109}/A_{1760} and was expressed as follows:

$$Y_{POSS} = 0.049(A_{1109}/A_{1760}) - 0.0011 \quad (1)$$

Results and Discussion

Characterization of Nanocomposites. FTIR Spectra. FTIR was used to check the structures of the resulting PAS−POSS hybrid nanocomposites. Figure 2 shows the FTIR spectrum of PAS−POSS as well as those of pure POSS and PAS for comparison. The pure POSS shows a strong and symmetric Si−O−Si stretching absorption band at ∼1109 cm^{-1}, which is the characteristic absorption peak of silsesquioxane cages. The PAS shows two characteristic absorptions at 1763 and 1216 cm^{-1}, which are assigned as the carbonyl stretching vibration and the strong Ph−O stretching absorption, respectively. The peaks at ∼1500 cm^{-1} come from the skeletal vibration of aromatic rings. The stretching absorption bands of methylene and methine groups are located at ∼2900 cm^{-1}. The IR spectrum of the PAS−POSS is very similar to that of the PAS except that a sharp and strong Si−O−Si stretching peak appear at ∼1109 cm^{-1} in all PAS−POSS nanocomposites. The consistent presence of this Si−O−Si stretching peak confirms that the POSS cage is truly incorporated into the resulting hybrid nanocomposites since the purification procedure for hybrids has ensured thorough removal of unreacted POSS macromers.

By detecting A_{1109}/A_{1760} values of the PAS−POSS hybrid nanocomposites, POSS molar contents in the hybrids were calculated on the basis of the calibration curve (Figure 1), and the results are shown in Table 1. Table 1 tells us that the molar fraction of POSS in the nanocomposites increases with the POSS feed ratio, which is consistent with our previous research,[29] implying that the contents of POSS in the hybrids can be effectively controlled by varying the POSS feed ratio.

^{1}H NMR Spectra. Since PAS−POSS hybrid nanocomposites are soluble in most common solvents, their structures can therefore be characterized by the solution ^{1}H NMR spectra. Figure 3 shows ^{1}H NMR spectra of POSS, PAS, and PAS−POSS in *d*-chloroform solvent. For pure POSS macromer, the multiple resonance peaks of vinyl protons are observed around ∼6.03 ppm because of the coupling of hydrogen protons. In the pure PAS, the broad resonance bands at 7.09 and 6.58 ppm are attributed to the aromatic protons. The band at 2.25 ppm is the characteristic peak of the methyl proton adjacent to the acyl group. The spectrum of PAS−POSS is very similar to that of the pure PAS, except that there is a wide resonance nearby 6 ppm, which belongs to the unreacted vinyl protons of POSS cage. The resonance bands of methine and methylene protons from the reacted vinyl groups of POSS segments overlap from 0.7 to 2.0 ppm with those of methine and methylene protons in the PAS backbones.

The chemical shift of 2.25 ppm in the PAS is attributed to the carbonyl-substituted methyl proton peak, while the POSS moiety does not possess any resonance band in this region. Similarly, POSS shows proton resonance peaks of unreacted vinyl groups at ∼6.0 ppm, while PAS exhibits no NMR resonance peaks in this

Table 1. Effect of POSS Feed Ratio on the Properties of PAS−POSS Nanocomposites

	POSS (mol %)									
no.	feed mole ratio	product mole ratio[a]	yield (wt %)	M_w[b] ($\times 10^3$ g/mol)	M_n ($\times 10^3$ g/mol)	PDI	x	T_g[c]	T_{dec}[d]	char yield (%)
1	0.00	0.00	71.2	43.7	31.6	1.38	/	123.2	369.4	0
2	0.35	0.14	65.5	39.1	22.2	1.76	0.0	122.0	387.6	3
3	1.40	1.34	59.7	43.5	25.1	1.73	0.4	127.7	379.3	3
4	2.58	1.85	55.4	37.3	20.5	1.82	1.3	130.9	410.6	13
5	6.21	3.86	50.3	24.0	14.6	1.65	2.7	135.9	417.7	22
6	8.10	4.68	47.8	28.9	16.4	1.76	3.6	138.4	423.9	25

[a] Data were obtained based on the IR standard curve. [b] Data were determined by GPC using the PS standard curve. [c] Data were gathered on the second melting at a heating rate of 10 °C/min. [d] Data were taken to be the temperature at 5% weight loss.

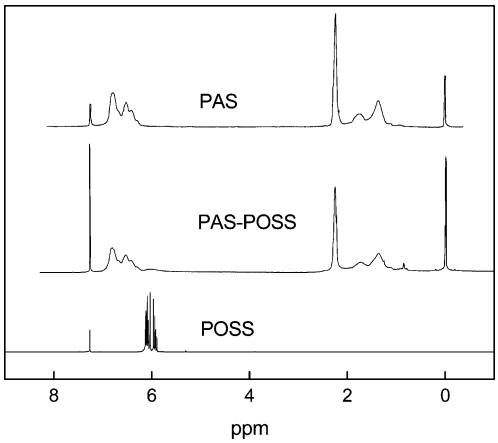

Figure 3. ^{1}H NMR spectra of POSS, PAS, and PAS−POSS.

region. Therefore, we can estimate the number of unreacted vinyl groups (x) from POSS segments based on the ^{1}H NMR spectra and the POSS content in the hybrids using the following formula:

$$\text{POSS (mol)\%} = \frac{A_{6.0}/3x}{A_{6.0}/3x + A_{2.25}/3} \times 100\% \qquad (2)$$

In formula 2, $A_{6.0}$ and $A_{2.25}$ represent the absorbance peak area at 6.0 and 2.25 ppm, respectively. On the basis of the detected peak areas, the x values are calculated (see Table 1). From Table 1, we find that averagely 4−8 vinyl groups from POSS macromers participated in the copolymerization. The ^{29}Si NMR spectrum also shows that most of the eight vinyl groups on each POSS macromer were consumed in the reaction since the peak area at −66 ppm (representing the reacted vinyl groups) is much bigger than that at −79 ppm (representing the unreacted vinyl groups, see Figure 4). These observations confirm that the resulting hybrid nanocomposites are not linear molecules. We tested the solubility of the hybrids in various solvents such as THF, $CHCl_3$, DMF, and so on. The results indicated that these hybrids could dissolve in most of the common solvents. This fact makes us believe that the synthesized hybrid nanocomposites are possibly of star-type structure rather than of network structure since network nanocomposites are virtually insoluble in any solvent.

Gel Permeation Chromatograph (GPC) Analyses. All results of GPC analyses are listed in Table 1. The molecular weight (M_w) of the mother polyacetoxystyrene is 43.7×10^3 with a polydispersity of 1.38. All the nanocomposites with various molar ratios of acetoxystyrene/POSS show a little higher polydispersity than pure polyacetoxystyrene. The slight disparity in

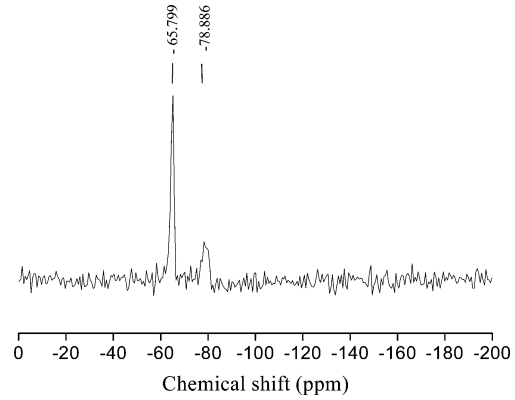

Figure 4. ^{29}Si NMR spectrum of PAS−POSS. δ: −66 ppm (CH_2CH-Si), −79 ppm ($CH_2=CH-Si$).

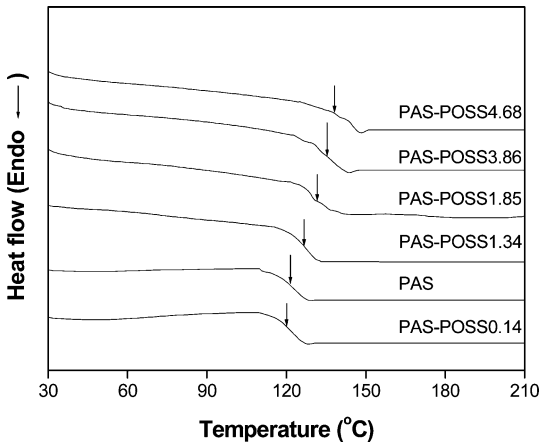

Figure 5. DSC thermograms of PAS and PAS−POSS.

polydispersity among PAS−POSS nanocomposites illustrates that the POSS content make a little impact on the molecular distribution when POSS were incorporated into the polyacetoxystyrene backbones. We all know that molecular weights of star polymers measured by GPC with linear monodispersed polystyrene as the standard are not accurate enough because of their big difference in structures, and since star polymers have smaller thermodynamic volume than linear ones, the real molecular weights of star polymers are actually higher than what measured by GPC. Fortunately, this systematic error does not influence the parallel comparison among PAS−POSS nanocomposites.

Thermal Properties and T_g Enhancement Mechanism. The DSC and TGA techniques were employed to investigate the thermal properties of the PAS−POSS hybrids, and FTIR was used to discuss the T_g enhancement mechanism. Figure 5 shows the DSC thermograms of various PAS−POSS hybrids and pure PAS. The PAS homopolymer has a T_g at 123.2 °C. When 0.14

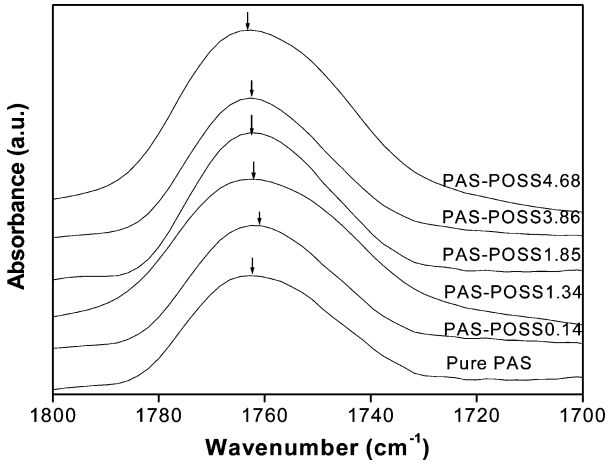

Figure 6. Expanded FTIR spectra in the regions ranging from 1800 to 1700 cm^{-1} of pure PAS and PAS−POSS polymers.

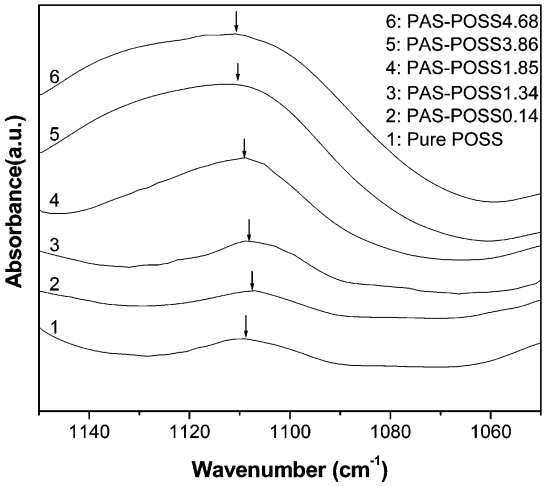

Figure 7. Expanded FTIR spectra in the regions ranging from 1150 to 1050 cm^{-1} of POSS and PAS−POSS hybrids.

mol % POSS was incorporated into the PAS polymers, T_g slightly decreased to 122.0 °C. This T_g change was expected because similar phenomena were found in our previous researches on linear PAS−POSS nanocomposites prepared by the polymerization of acetoxystyrene and heptaisobutylstyryl-POSS.[29−32] It proves that the incorporation of a relatively small amount of POSS macromers into homopolymers does not increase the T_g of the mother polymers but actually reduces its T_g owing to diluent effect of the bulky POSS cages, which weaken the dipole−dipole interaction between PAS chains and decrease the self-aggregation interaction of PAS molecules. However, when 1.34 mol % POSS is embedded into the polymer system, a T_g at 127.7 °C is observed, which is 4.5 °C higher than that of the mother PAS. The T_g of the PAS−POSS further increases with the increase of the POSS content. When the mole percentage of POSS in the hybrid reached 4.68%, the PAS−POSS nanocomposite shows a high T_g at 138.4 °C. A new effect other than diluent must exist when the mole percent of POSS in the hybrids is higher than 1.34%. To reveal the T_g change mechanism involved in these PAS−POSS hybrids, the characterization of their FTIR spectra ranging from 1800 to 1700 cm^{-1} for the pure PAS and various PAS−POSS nanocomposites is shown in Figure 6.

The mother PAS shows a characteristic carbonyl vibration band centered at 1760 cm^{-1}. When 0.14 mol % POSS is incorporated into the PAS, this maximum absorption shifts slightly toward lower frequency (lower wavenumber). However, when the POSS content is more than 1.34%, this maximum absorption tends to shift to higher frequency gradually. For example, the carbonyl maximum absorption peak shifts to 1765 cm^{-1} in the PAS−POSS4.68. Cheam[33] studied the relationship between the dipole interaction potential (V_{dd}) and the FTIR vibration frequency shift (Δv_i), which is expressed as follows:

$$\Delta v_i = \frac{V_{dd}}{hc} \tag{3}$$

The frequency shift is much related to the strength of dipole interaction. The absorbance frequency will increase with the enhancement of dipole interaction and decrease with the weakening of dipole interaction. Painter[34] studied the interaction potential between two dipoles, A and B, which is expressed in the following formula:

$$V_{dd} = -\mu_A\mu_B[\hat{e}_A\hat{e}_B - 3(\hat{e}_A r_{AB})(\hat{e}_A - r_{AB})]/{r_{AB}}^3 \tag{4}$$

where $\hat{e}$ is a unit vector describing the direction of the dipole moment and r_{AB} is the distance between the centers of the dipoles. From formula 4, we know that the increase of the distance between the centers of the dipoles will lead to the drop of the dipole interaction. With this theory and the FTIR spectra, we can well explain the T_g change of the nanocomposites. When a relatively small amount of POSS is incorporated into the PAS, POSS acts as a diluent block to enlarge the distance between PAS molecular chains and results in the decrease of their dipole−dipole interaction. This inference is verified by the frequency shift toward lower value in the FTIR spectra with the incorporation of 0.14 mol % POSS. However, with the further increase of POSS content, the dipole−dipole interaction between POSS and the polar carbonyl of PAS species increases, and this interaction increase tends to play a dominant role over the diluent effect of POSS cages. This dipole interaction increase is also reflected in the frequency shift toward higher value of the carbonyl vibration absorption when the content of POSS is more than 1.34 mol % in the hybrids. As a result, the observed T_g's of the PAS−POSS hybrids show a tendency of first decrease and then increase with the increase of the POSS content (Table 1).

To further explain the T_g enhancement mechanism of the PAS−POSS nanocomposites, the expanded FTIR spectra of various PAS−POSS hybrids in the region from 1150 to 1050 cm^{-1} are shown in Figure 7, from which we can observe the change of characteristic stretching absorption band of POSS moieties in the hybrids. The Si−O−Si vibration peak, centered at 1109 cm^{-1}, shifts toward lower frequency with a small amount of POSS in the hybrid system. For example, the peak maximum is located at 1107 cm^{-1} with 0.14 mol % POSS. This result is due to the dipole−dipole interaction occurred between the POSS cages and the PAS carbonyls. However, when POSS content in the hybrid is higher than 1.34 mol %, the POSS−POSS interaction begins to increase. This accounts for the shift of POSS characteristic absorption band toward higher frequency. Since the bulky POSS molecules strongly influence the polymer chain motion, the POSS−POSS interaction

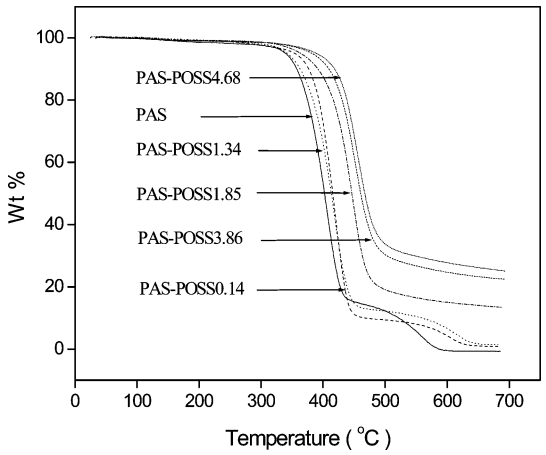

Figure 8. TGA thermograms of PAS and PAS−POSS.

provides another contribution to the T_g increase besides the POSS−PAS dipole interaction in the hybrids, especially when the POSS content is higher. As mentioned above, POSS plays a role of diluent to lower the PAS dipole−dipole interaction at relatively lower POSS contents (less than 0.14 mol % POSS) and acts to increase the POSS−PAS and POSS−POSS interactions at relatively higher POSS contents (more than 1.34 mol % POSS). These two adverse and competitive effects account for the first decrease and then increase of T_g of the hybrid nanocomposites. A similar T_g change with the POSS content was also found in our previous study on linear PAS−POSS nanocomposites.[29−32] With the same POSS feed ratio, the star polymers we prepared in this paper have lower POSS mole percentages calculated by FTIR method in the hybrids but possess higher T_g than the linear polymers, which can be explained by the special structure of star polymers. In PAS−POSS star polymers, PAS chains are attached covalently to the POSS cores, and thus the motions of PAS segments are not as easy as either in the homogeneous PAS or in the linear PAS−POSS nanocomposites but actually hindered effectively by the POSS cores. Therefore, the chain segment motion of star PAS−POSS nanocomposites needs higher temperature. As a result, higher T_g's were observed in the star PAS−POSS hybrids than in the linear PAS−POSS hybrids at the same POSS content.

Figure 8 shows the TGA thermograms of various PAS−POSS hybrids and pure PAS. The temperatures of 5% weight loss (T_{dec}) and the char yield are recorded in Table 1. The pure PAS has a T_{dec} at 369.4 °C and has no remnant when the temperature reaches 700 °C. For PAS−POSS hybrids, the T_{dec} and char yield increase with the increase of POSS contents. For example, PAS−POSS0.14 has a T_{dec} at 387.6 °C (18.2 °C higher than pure PAS) and 3% char yield at 700 °C, while PAS−POSS4.68 has a T_{dec} at 423.9 °C and 25% char yield at 700 °C. The obvious improvement of thermal stability is rarely observed in linear PAS−POSS hybrids.[32] This fact also indicates that star nanocomposites have better thermal stability than the corresponding linear nanocomposites.

Conclusions

The nanoscale well-defined octavinyl-polyhedral oligomeric silsesquioxane (POSS) was incorporated into the polyacetoxystyrene system by common free-radical polymerization to yield PAS−POSS hybrids. The POSS content in the PAS−POSS hybrids can be adjusted simply by changing the POSS feed ratio. The PAS−POSS hybrid nanocomposites were characterized by FTIR, ^{1}H NMR, ^{29}Si NMR, and GPC, which proved that the resultant nanocomposites were of star structure. The thermal properties of the star PAS−POSS hybrid nanocomposites were studied by the DSC and TGA techniques. The FTIR spectra were employed to explain the T_g improvement mechanism, which indicates that the T_g improvement is associated with the aggregation of POSS particles and the dipole−dipole interaction between POSS and PAS molecules. The T_g decrease at lower POSS contents comes from the inert diluent effect of POSS macromers, which reduce the dipole−dipole interaction of the homogeneous PAS molecules. With the increase of POSS contents, the enhancement of the dipole−dipole interactions of POSS−POSS and POSS−PAS surpasses the decrease of the dipole−dipole interaction of PAS−PAS to result in the increase of the T_g's. The higher T_g's and better thermal stability were observed in the star PAS−POSS hybrids than in the linear PAS−POSS hybrids at the same POSS content.

Acknowledgment. This research was financially supported by the National Natural Science Fund of China (Grants 90206014 and 50472038), the Excellent Youth Fund of Anhui Province (Grant 04044060), and the Program for New Century Excellent Talents in Universities (NCET-04-0588) and the Award for High-level Intellectuals (Grant 2004Z027) from Anhui Province.

References and Notes

(1) Tsuchida, A.; Bolln, C.; Sernetz, F. G.; Frey, H.; Mulhaupt, R. *Macromolecules* **1997**, *30*, 2818.
(2) Haddad, T. S.; Lichtenhan, J. D. *Macromolecules* **1996**, *29*, 7302.
(3) Mather, P. T.; Jeon, H. G.; Romo-Uribe, A.; Haddad, T. S.; Lichtenhan, J. D. *Macromolecules* **1999**, *32*, 1194.
(4) Lichtenhan, J. D.; Otonari, Y. A.; Carri, M. J. *Macromolecules* **1995**, *28*, 8435.
(5) Romo-Uribe, A.; Mather, P. T.; Haddad, T. S.; Lichtenhan, J. D. *J. Polym. Sci., Part B: Polym. Phys.* **1998**, *36*, 1857.
(6) Lee, A.; Lichtenhan, J. D. *Macromolecules* **1998**, *31*, 4970.
(7) Lee, A.; Lichtenhan, J. D. *J. Appl. Polym. Sci.* **1999**, *73*, 1993.
(8) Lichtenhan, J. D.; Vu, N. Q.; Carter, J. A. *Macromolecules* **1993**, *26*, 2141.
(9) Shockey, E. G.; Bolf, A. G.; Jones, P. F.; Schwab, J. J.; Chaffee, K. P.; Haddad, T. S.; Lichtenhan, J. D. *Appl. Organomet. Chem.* **1999**, *13*, 311.
(10) Fu, B. X.; Zhang, W.; Hsiao, B. S.; Johansson, G.; Sauer, B. B.; Phillips, S.; Balnski, R.; Rafailovich, M.; Sokolov, J. *Polym. Prepr.* **2000**, *41*, 587.
(11) Fu, B. X.; Hsiao, B. S.; Pagola, S.; Stephens, P.; White, H.; Rafailovich, M.; Sokolov, J.; Mather, P. T.; Jeon, H. G.; Phillips, S.; Lichtenhan, J.; Schwab, J. *Polymer* **2001**, *42*, 599.
(12) Zheng, L.; Farris, R. J.; Coughlin, E. B. *Macromolecules* **2001**, *34*, 8034.
(13) Phillips, S. H.; Haddad, T. S.; Tomczak, S. T. *Curr. Opin. Solid State Mater. Sci.* **2004**, *8*, 21.
(14) Lichtenhan, J. D.; Otonari, Y. A.; Carr, M. J. *Macromolecules* **1995**, *28*, 8435.
(15) Zheng, L.; Kasi, R. M.; Farris, R. J.; Coughlin, E. B. *J. Polym. Sci., Part A: Polym. Chem.* **2002**, *40*, 885.
(16) Zheng, L.; Farris, R. J.; Coughlin, E. B. *J. Polym. Sci., Part A: Polym. Chem.* **2001**, *39*, 2920.
(17) Bharadwaj, R. K.; Berry, R. J.; Farmer, B. L. *Polymer* **2000**, *41*, 7209.
(18) Jeon, H. G.; Mather, P. T.; Haddad, T. S. *Polym. Int.* **2000**, *49*, 453.
(19) Pyun, J.; Matyjaszewski, K. *Macromolecules* **2000**, *33*, 217.
(20) Choi, J.; Harcup, J.; Yee, A. F.; Zhu, Q.; Laine, R. M. *J. Am. Chem. Soc.* **2001**, *123*, 11420.
(21) Sellinger, A.; Laine, R. M. *Macromolecules* **1996**, *29*, 2327.

(22) Lucke, S.; Stoppek-Langner, K.; Kuchinke, J.; Krebs, B. *J. Organomet. Chem.* **1999**, *584*, 11.
(23) Fasce, D. P.; Williams, R. J. J.; Balsells, R. E.; Ishikawa, Y.; Nonami, H. *Macromolecules* **2001**, *34*, 3534.
(24) Fasce, D. P.; Williams, R. J. J.; Mechin, F.; Pascault, J. P.; Liauro, M. F.; Petiaud, R. *Macromolecules* **1999**, *32*, 4757.
(25) Zhang, C. X.; Babonneau, F.; Bonhomme, C.; Laine, R. M.; Soles, C. L.; Hristov, H. A.; Yee, A. F. *J. Am. Chem. Soc.* **1998**, *120*, 8380.
(26) Tamaki, R.; Tanaka, Y.; Asuncion, M. Z.; Choi, J.; Laine, R. M. *J. Am. Chem. Soc.* **2001**, *123*, 12416.
(27) Ni, Y.; Zheng, S. X. *Chem. Mater.* **2004**, *16*, 5141.
(28) Harrison, P. G.; Hall, C.; Kannengiesser, R. *Main Group Met. Chem.* **1997**, *20*, 515.
(29) Xu, H. Y.; Kuo, S. W.; Lee, J. S.; Chang, F. C. *Macromolecules* **2002**, *35*, 8788.
(30) Xu, H. Y.; Kuo, S. W.; Huang, C. F.; Chang, F. C. *J. Appl. Polym. Sci.* **2004**, *91*, 2208.
(31) Xu, H. Y.; Kuo, S. W.; Lee, J. S.; Chang, F. C. *Polymer* **2002**, *43*, 5117.
(32) Xu, H. Y.; Kuo, S. W.; Huang, C. F.; Chang, F. C. *J. Polym. Res.* **2002**, *9*, 239.
(33) Cheam, T. C.; Krimm, S. *Chem. Phys. Lett.* **1984**, *107*, 613.
(34) Painter, P. C.; Pehlert, G. J.; Hu, Y.; Coleman, M. M. *Macromolecules* **1999**, *32*, 2055.

MA0516687